Research Square

Preprints are preliminary reports that have not undergone peer review.
They should not be considered conclusive, used to inform clinical practice,
or referenced by the media as validated information.

Towards the development of aluminum-based cellular eco-mortar containing recycled granite sand: thermophysical and mechanical properties

Philbert NSHIMIYIMANA

philbert.nshimiyimana@2ie-edu.org

Institut International d'Ingénierie de l'Eau et de l'Environnement (Institut 2iE)

Yasmine Binta TRAORE

Université Yembila Abdoulaye TOGUYENI (UYAT) (ex-université de Fada N'Gourma), Ecole Supérieure d'Ingénierie (ESI)

Arnaud Louis Sountong-Noma OUEDRAOGO

Institut International d'Ingénierie de l'Eau et de l'Environnement (Institut 2iE)

Mohamed Naman CONDE

Institut International d'Ingénierie de l'Eau et de l'Environnement (Institut 2iE)

Cesaire HEMA

Institut International d'Ingénierie de l'Eau et de l'Environnement (Institut 2iE)

Nafissatou SAVADOGO

Université Yembila Abdoulaye TOGUYENI (UYAT) (ex-université de Fada N'Gourma), Ecole Supérieure d'Ingénierie (ESI)

Adamah MESSAN

Institut International d'Ingénierie de l'Eau et de l'Environnement (Institut 2iE)

Article

Keywords: cellular mortar, aluminum powder, recycled granite sand, physical property, mechanical property, thermal property

Posted Date: June 19th, 2026

DOI: https://doi.org/10.21203/rs.3.rs-9910252/v1

License: This work is licensed under a Creative Commons Attribution 4.0 International License.
Read Full License

Additional Declarations: No competing interests reported.

Towards the development of aluminum-based cellular eco-mortar containing recycled granite sand: thermophysical and mechanical properties

Philbert NSHIMIYIMANA [1] *, Yasmine Binta TRAORE [2], Arnaud Louis Sountong-Noma OUEDRAOGO [1], Mohamed Naman CONDE [1], Cesaire HEMA[1], Nafissatou SAVADOGO [2], Adamah MESSAN [1]

[1] Laboratoire Eco-Matériaux et Habitats Durables (LEMHaD), Institut International d'Ingénierie de l'Eau et de l'Environnement (Institut 2iE), Ouagadougou, Burkina Faso

[2] Université Yembila Abdoulaye TOGUYENI (UYAT) (ex-université de Fada N'Gourma), Ecole Supérieure d'Ingénierie (ESI), Département de Génie Civil, Fada N'Gourma, Burkina Faso.

* Corresponding author: Philbert NSHIMIYIMANA philbert.nshimiyimana@2ie-edu.org

ABSTRACT

This study focuses on the design of an eco-friendly cellular mortar for the Sudano–Sahelian hot and dry climate of Burkina Faso, containing aluminum powder and sand from the recycling of granite waste. Mortars containing two types of sand (natural sand: NS and recycled granite sand: GS) were tested with varying aluminum powder (Al) dosages (0%, 0.5%, and 1%). The sand/cement (S/C) ratios were 4, 3, and 2, and the water/cement (W/C) ratios were 0.6 to 1.2. Experiments were conducted to evaluate the physical, mechanical, and thermal properties of fresh and hardened mortar. The results show improvements in the thermophysical properties with increasing aluminum powder content and W/C ratio and decreasing S/C ratio. Adding 0 to 1% Al in the mortar, containing an S/C of 2 at a W/C of 1.2, increased its linear swelling in the fresh state up to 61%, reducing the bulk density in hardened state by 44% from 1785 to 1003 kg/m³ with GS. On the contrary, a swelling of only 50% and a reduction of density by 35% from 1796 to 1168 kg/m³ were recorded with NS, owing to the formation of cellular pores. This resulted in a decrease in thermal conductivity by 90% (0.93 to 0.09 W/m.K) with GS and by 71% (1.25 to 0.36 W/m.K) with NS, towards insulating performance. However, the compressive strength decreased from 15.5 to 2.4 MPa (-84%) with GS and from 10.3 to 7.1 MPa (-31%) with NS, with the increase in porosity. These cellular mortars offer promising alternatives to ordinary mortar in terms of lightweight, quasi-insulating properties, and potential reduction in environmental impacts from the recycling of granite sand.

Keywords : cellular mortar; aluminum powder; recycled granite sand, physical property; mechanical property; thermal property

INTRODUCTION

Today, the concrete industry is still experiencing strong growth owing to population explosion and the need for infrastructure, especially in developing countries. In the coming years, the global demand for construction will surge. Meeting this demand is challenging, as it requires more construction materials; however, it offers opportunities to explore alternative solutions (UN-Habitat, 2022)(Maza et al., 2023) (Habsya et al., 2018; Karri et al., 2018).

In the hot and dry Soudano-Sahelian climate, such as that of Burkina Faso, ordinary hydraulic concrete is not only environmentally unsustainable (Nouhoun et al., 2025), economically unaffordable (Nshimiyimana et al., 2025), but also unsuitable for achieving the required hygrothermal performance (Prozuments et al., 2025)(Hema et al., 2021). Several studies have demonstrated the thermal, structural, and durability potentials of alternative materials (Hema et al., 2020)(Ramadji et al., 2020). However, there is an urgent need to develop alternative materials for constructing sustainable and comfortable housing (Ouédraogo et al., 2022)(Hema et al., 2021)(Ouedraogo et al., 2022). The transition toward low-carbon construction materials would be highly supported by lightweight, regenerative, and thermally efficient materials capable of reducing dead loads, environmental impacts, and embodied and operational energy of buildings.

Conventional hydraulic mortars have a density in the range of 1800–2200 kg/m³ and thermal conductivity above (1.5-2 W/mK)(Talebi et al., 2020), limiting their suitability in hot and energy-intensive climates (Talebi et al., 2020). In contrast, cellular and foamed mortars achieve significantly lower density and better thermal performance by generating controlled pore structures within the matrix, making them attractive solutions for sustainable building applications (Liu et al., 2024)(Mohamed et al., 2024). Unlike conventional mortars, cellular mortars are light, with a density ranging in 350-1850 kg/ m³ (Karri et al., 2018)(Liu et al., 2024) allowing for a relatively low thermal conductivity (<0.2 W/mK)(Ganesan et al., 2015; Habsya et al., 2018).

Aluminum powder (Al) is a chemical foaming agent used to produce cellular cementitious composites. In alkaline media, metallic Al reacts with hydroxyl ions (OH^-) to generate hydrogen gas (H_2), producing interconnected pores depending on the Al fineness, water availability, slurry viscosity, and boundary constraints. Recent studies have described pore evolution beginning with nucleation and bubble growth, followed by coalescence and stabilization or collapse, depending on the slurry rheology and gas formation rates (Dhasindrakrishna et al.,

2021)(Mohamed et al., 2024). The foam stability is strongly influenced by the viscosity and yield-stress behavior of the slurry. Lower viscosity allows bubbles to migrate and escape, whereas higher viscosity stabilizes the pore walls but risks irregular coalescence. Additives such as superplasticizers or mechanical activation can modify rheology and improve the uniformity of the pore system. Closed-cavity conditions also play a critical role: foams expanded in constrained systems exhibit smaller and more uniform sizes than those formed under free expansion (Dhasindrakrishna et al., 2021)(Liu et al., 2024)(Mohamed et al., 2024).

The most sought-after performances of cellular concrete, such as light weight and thermal behavior, are governed by its density, porosity, pore connectivity, and aggregate type. Numerous studies have confirmed that increasing the pore volume or using lightweight fillers reduces the thermal conductivity to 0.1–0.3 W/m·K, which is typical of insulating mortars (Liu et al., 2024)(Gencel et al., 2022)(Al-Ani et al., 2025). Granular waste materials such as expanded perlite, pumice, cork, or recycled polymers also reduce the density and thermal conductivity, although they are often accompanied by diminished mechanical strength (Akkouri et al., 2022)(Gencel et al., 2022)(Abdellatief et al., 2024). Therefore, the thermal-mechanical trade-offs are common in cellular materials: lower density improves insulation but weakens the solid skeleton, whereas micro-fillers and reactive fines can partially compensate for strength by densifying the matrix or contributing to secondary hydration (Liu et al., 2024)(Zafar et al., 2020)(Abhilasha et al., 2023). Additionally, the correlation between the pore structure and thermal conductivity is well documented: smaller, more uniform, and closed pores lead to higher insulation (Chen et al., 2021).

Furthermore, the cutting and aggregate industries generate a significant amount of granite waste. Recent reviews have identified granite waste as one of the most promising industrial byproducts for incorporation in mortars and concrete owing to its mineralogy, angular morphology, and microfiller potential (Saxena et al., 2022)(Gupta & Vyas, 2018)(Al Ismaeel et al., 2026). This granite sand can enhance strength, densify the microstructure, and refine the pore distribution owing to its ability to fill voids and support C–S–H formation (Zafar et al., 2020). Studies on both cementitious and geopolymer matrices have reported increased compressive strength and durability up to an optimum substitution threshold, before excessive fines increase the water demand or porosity (Saxena et al., 2022)(Ramadji et al., 2020). Beyond the engineering benefits, the incorporation of recycled granite waste substantially reduces environmental impacts and costs, offering improved life-cycle performance (Ramadji et al., 2020). In cellular systems, granite waste has been successfully used in autoclaved aerated concrete (AAC), where it improves mechanical properties, stabilizes pore structure, and

increases resistance to acid attack (Abhilasha et al., 2023; Zafar et al., 2020). These advantages suggest that recycled granite sand can synergize with aluminum-based foaming, contributing to both the filler effects and improved pore stability.

Although significant research exists on aluminum-based foaming and the valorization of granite waste in mortars, studies combining both materials in an eco-mortar system remain scarce, especially in the local context where granite materials are widely exploited. The potential synergy of Al-induced porosity for lightweight insulation and granite sand, compared to natural river sand, has not been fully explored. This study addresses this gap by evaluating the thermophysical and mechanical properties of an aluminum-based cellular mortar incorporating recycled granite sand, positioning it within ongoing efforts to develop high-performance, low-carbon materials.

MATERIALS AND METHODS

Materials

Portland cement CEM II/BM (PL) 42.5, produced by CIMBURKINA (Burkina Faso), was used as the binder for the concrete. Two types of fine aggregates (sand) with a particle size of 0/2 mm were used: natural river sand (NS) and recycled sand derived from crushed granite residue (GS). Both aggregates were free of silt and clay content. Tap water was used in all mixes, and no plasticizer or admixture was incorporated. Aluminum powder was used as a chemical foaming agent. The product was supplied by Laborladen (Germany) with a purity of 99.8% and particle size below 45 µm. Figure 1 shows the materials used in this study.



a b c d

Figure 1. Materials : a) cement, b) aluminum powder, c) natural sand, d) recycled granite sand

Mixtures design and specimens preparation

Two foamed mixes with 0.5% and 1% Al by cement mass were prepared for each sand type. Sand-to-cement ratios (S/C) of 2, 3, and 4 were investigated, with corresponding W/C ratios of 0.6–1.2. Control mixes (0% Al) were prepared for each S/C and W/C ratio. The mixing proportions are summarized in Table I.

Cement and sand were first dry-mixed until homogeneity was achieved. Water and aluminum powder were then added and mixed until a homogeneous slurry was obtained. The fresh mortar was cast into prismatic molds (40 × 40 × 160 mm³) in two layers, each compacted with 60 impacts using an impact driver for the mixes with low workability. The molds were covered and stored at ambient temperature (30±5°C) for 24 h to allow hydration of cement, foam formation and expansion, and setting. The specimens were demolded and cured in water for 28 d until testing. Various tests were performed on dry samples to characterize their physical, mechanical, and thermal properties (Figure 2).

Table I: Designs of cellular mortars

Sand/Cement S/C	**Water/Cement W/C**	**Cement C (g)**	**Sand S (g)**	**Water W (g)**	**Aluminum Powder A, at 0.5% (g)**	**Aluminum Powder A, at 1% (g)**
4	0.7	2000	4000	1400	10	20
3	0.6	2250	6750	1350	11.25	22.25
	0.8	2250	6750	1800	11.25	22.25
	1	2250	6750	2250	11.25	22.25
2	0.6	3000	6000	1500	15	30
	0.8	3000	6000	2400	15	30
	1	3000	6000	3000	15	30
	1.2	3000	6000	3600	15	30

Characterization of physical properties

Swelling was measured as the relative linear increase in height between the initial and expanded states, expressed as a percentage. The bulk density (ρd, kg/m³) was determined using hydraulic weighing. The dry mass (M_dry) was obtained after oven-drying to a constant mass. The saturated masses weighed in water (M_sat.water) and air (M_sat.air) were recorded after 24 h of immersion. The density of the samples was calculated considering the density of water ($\rho water$) of 1000 kg/m^3 (Equation 1). Water-accessible porosity (P, %) was calculated from the saturated and dry masses using Equation 2, where M_air is the saturated mass weighed in air, M_dry is the dry mass, and M_water is the saturated mass weighed in water. Tests were performed on at least three specimens per design.



a b c

Figure 2. Samples for testing: a) swelling, b) mechanical c) thermal properties

Characterization of mechanical properties

Mechanical tests were conducted after 28 days of curing, following 24 h of surface drying, and measured on three prism specimens per design using an automated hydraulic press. The three-point flexural strength (Rf, MPa) was calculated using equation 3, where Fl is the breaking load (N), b is the section side length (40 mm), and l is the span between the supports (100 mm). The compressive strength (Rc, MPa) was calculated from the measurements of the six resulting half-prism specimens (Equation 4), where Fc is the failure load (N) applied over a 40 × 40 mm² area.

Characterization of thermal properties

The thermal effusivity (E, J/m²KS$^{1/2}$) and volumetric heat capacity (Cv, J/m³·K) were measured under dry conditions using a DEsProTherm "thermal property estimation device" on specimens of 60 × 40 × 10 and 60 × 40 × 20 mm³. Thermal conductivity ($\lambda, W/m.K$ was derived from the effusivity and volumetric heat capacity using equation 5.

$$\rho d = \frac{Mdry * \rho water}{Msat.air - Msat.water} \quad \text{Equation 1}$$

$$P = \frac{Msat.air - Mdry}{Msat.air - Msat.water} * 100 \quad \text{Equation 2}$$

$$Rf = \frac{1.5 * Fl * l}{b^3} \quad \text{Equation 3}$$

$$Rc = \frac{Fc}{40x40} \quad \text{Equation 4}$$

$$\lambda = \frac{E^2}{Cv} \quad \text{Equation 5}$$

RESULTS

Physical Properties

Evolution of swelling

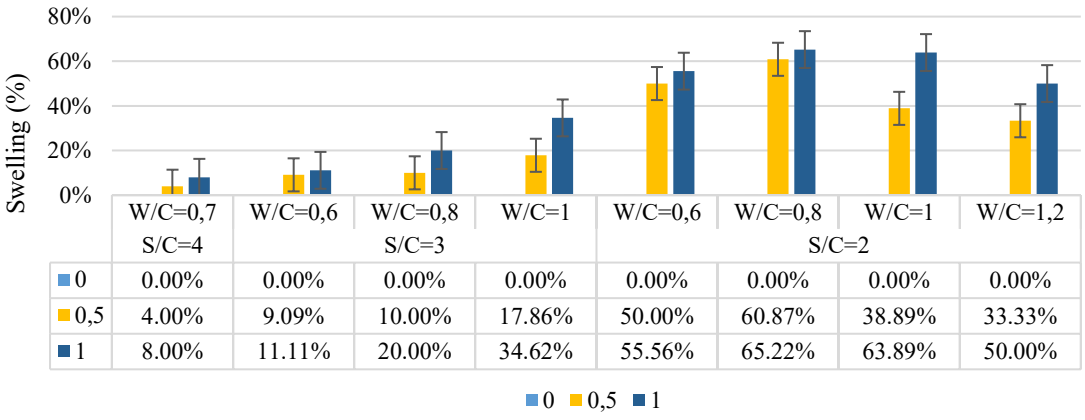
The swelling of cellular mortars incorporating natural sand and recycled granitic sand (Figure

3 and Figure 4) depended consistently on the aluminum powder dosage, W/C ratio, and S/C ratio. Swelling was absent in the control mixtures (0% Al) and increased progressively with the addition of aluminum, reaching its highest value at 1%.

For natural sand, the swelling at 0.5% aluminum ranged from 4 to 60.87%, depending on the mix composition. At 1%, the values ranged from 8.00 to 65.22%, with the maximum recorded at W/C=0.8 and S/C=2 (65.22%). The lowest values occurred at W/C=0.7 and S/C=4 (8.00%), reflecting the combined influence of low water content and high sand-to-cement ratio that limited the swelling behavior.

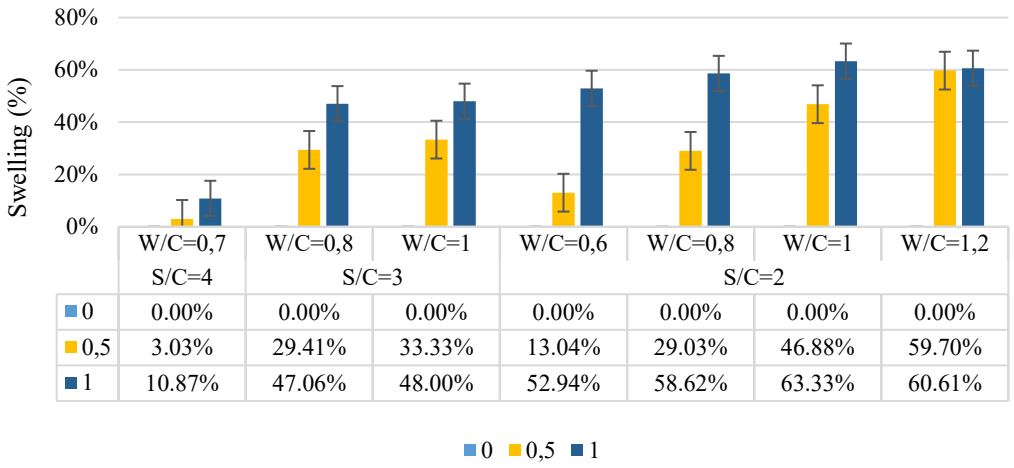
For recycled granitic sand, at 0.5%, the values of swelling range from 3.03 to 59.70%, with the maximum at W/C=1.2, S/C=2. At 1%, swelling ranged from 10.87 to 63.33%, with the highest values at W/C=0.8–1.2 and S/C=2.

The swelling was consistently comparable for granite and natural sand at equivalent aluminum content. The difference was most pronounced at a high W/C ratio (high water content) and low S/C ratio (high cement content), where granite sand significantly overperformed natural sand with higher swelling.



	W/C=0,7 S/C=4	W/C=0,6	W/C=0,8 S/C=3	W/C=1	W/C=0,6	W/C=0,8 S/C=2	W/C=1	W/C=1,2
0	0.00%	0.00%	0.00%	0.00%	0.00%	0.00%	0.00%	0.00%
0,5	4.00%	9.09%	10.00%	17.86%	50.00%	60.87%	38.89%	33.33%
1	8.00%	11.11%	20.00%	34.62%	55.56%	65.22%	63.89%	50.00%

Figure 3: Swelling with natural sand



	W/C=0,7 S/C=4	W/C=0,8 S/C=3	W/C=1 S/C=3	W/C=0,6 S/C=2	W/C=0,8 S/C=2	W/C=1 S/C=2	W/C=1,2 S/C=2
0	0.00%	0.00%	0.00%	0.00%	0.00%	0.00%	0.00%
0,5	3.03%	29.41%	33.33%	13.04%	29.03%	46.88%	59.70%
1	10.87%	47.06%	48.00%	52.94%	58.62%	63.33%	60.61%

Figure 4: Swelling with granitic sand

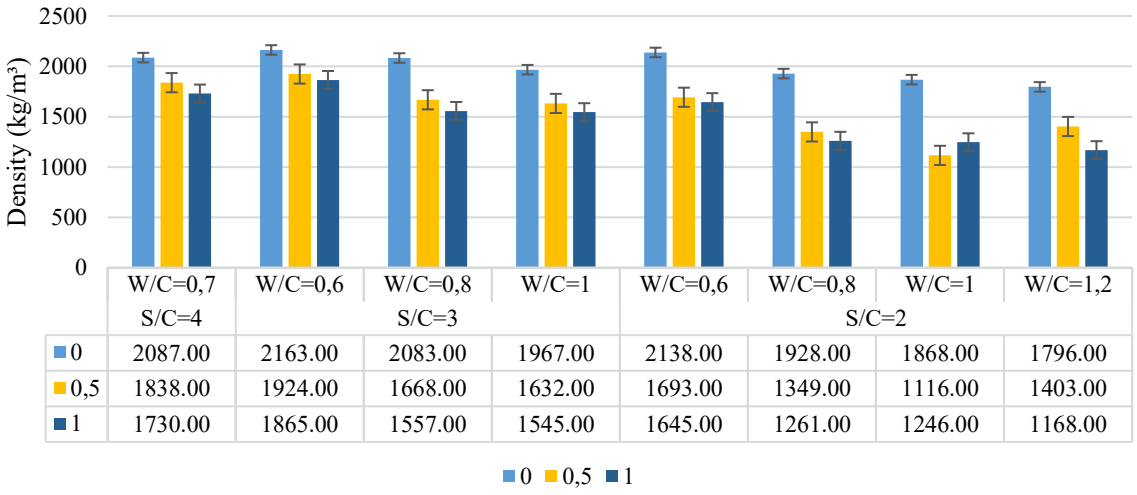
Evolution of bulk density

The bulk density decreased systematically with increasing aluminum content for both sand types (Figure 5 and Figure 6). For all mix proportions, the density decreased progressively from 0% to 0.5% to 1% aluminum, with the magnitude of reduction depending on the W/C and S/C ratios.

For natural-sand mixtures, the values of density at 0% aluminum ranged from 1967 to 2163 kg/m³ at S/C=4 (W/C=0.7) and from 1868 to 2138 kg/m³ at S/C=2 (W/C=0.6 to 1.2). The wider range at S/C=2 reflects the broader W/C span tested for that series. At 0.5% aluminum, density drops to 1632–1924 kg/m³, and further to 1545–1865 kg/m³ at 1%. The highest reductions occur at W/C=1.2, S/C=2, where density decreased from 1796 kg/m³ (0%) to 1168 kg/m³ (1%), a reduction of 35%.

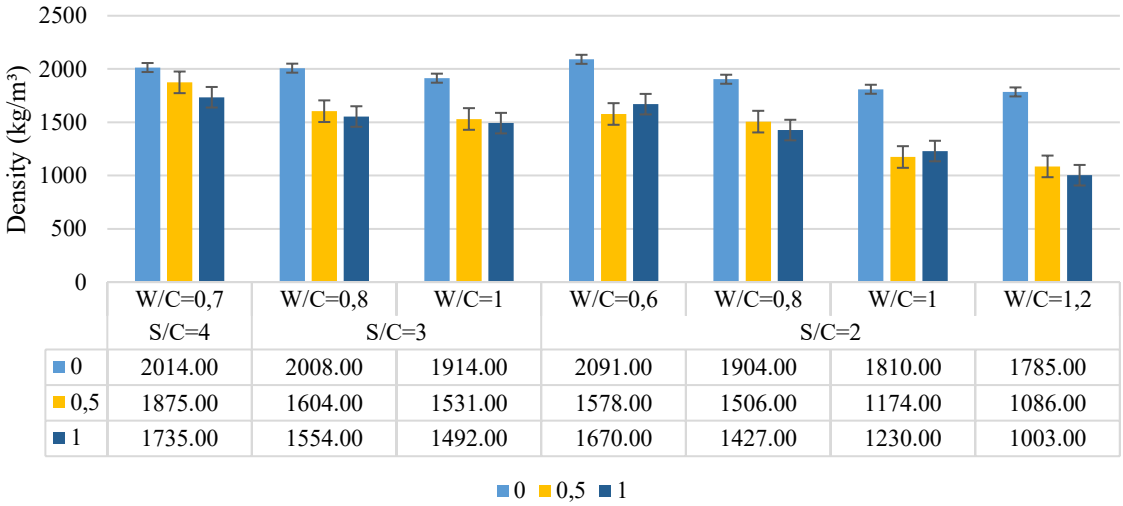
For the granitic-sand mixtures, the same trend was observed, with consistently lower values of final density. The values for the control ranged from 1914 to 2091 kg/m³ at S/C=3 and from 1785 to 2014 kg/m³ at S/C=2. The density decreased to 1531–1875 kg/m³ at 0.5% aluminum and further to 1492–1735 kg/m³ at 1%. The minimum density across all designs was 1003 kg/m³, recorded at a W/C of 1.2, S/C of 2, and 1% aluminum, reflecting a 44% reduction from the 0% Al reference of 1785 kg/m³.

For equivalent mix proportions and aluminum dosages, the recycled granitic sand consistently produced a lower bulk density than the natural sand. The difference was largest at high W/C and low S/C ratios.



	W/C=0,7 S/C=4	W/C=0,6 S/C=3	W/C=0,8 S/C=3	W/C=1 S/C=3	W/C=0,6 S/C=2	W/C=0,8 S/C=2	W/C=1 S/C=2	W/C=1,2 S/C=2
0	2087.00	2163.00	2083.00	1967.00	2138.00	1928.00	1868.00	1796.00
0,5	1838.00	1924.00	1668.00	1632.00	1693.00	1349.00	1116.00	1403.00
1	1730.00	1865.00	1557.00	1545.00	1645.00	1261.00	1246.00	1168.00

Figure 5: Density with natural sand



	W/C=0,7 S/C=4	W/C=0,8 S/C=3	W/C=1 S/C=3	W/C=0,6 S/C=2	W/C=0,8 S/C=2	W/C=1 S/C=2	W/C=1,2 S/C=2
0	2014.00	2008.00	1914.00	2091.00	1904.00	1810.00	1785.00
0,5	1875.00	1604.00	1531.00	1578.00	1506.00	1174.00	1086.00
1	1735.00	1554.00	1492.00	1670.00	1427.00	1230.00	1003.00

Figure 6: Density with granitic sand

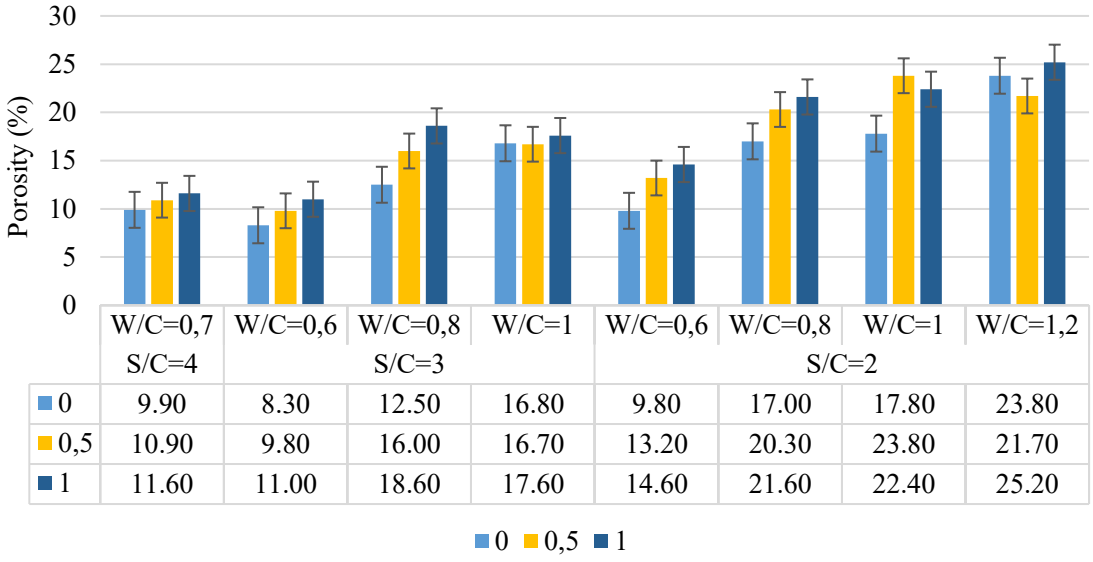
Evolution of porosity

Water-accessible porosity increased with the addition of aluminum powder and higher W/C ratios for both sand types (Figure 7 and Figure 8). The control mixtures (0% Al) exhibited the lowest porosity values, and the mixtures containing 1% Al displayed the highest values across all S/C and W/C conditions.

For natural sand, the porosity at 0% Al ranged from 8.3% (W/C=0.6, S/C=4) to 23.8% (W/C=1.2, S/C=2). At 0.5% Al, the values increased to 9.8–23.8%, with the most pronounced increments recorded at lower S/C ratios (high cement content). At 1% Al, the porosity reaches

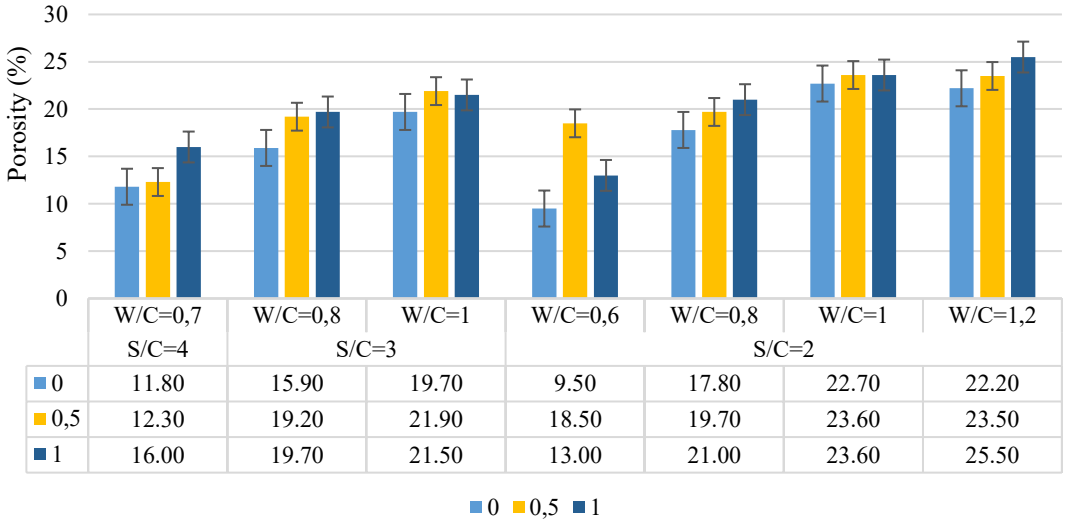
11–25.2%, with a maximum at W/C=1.2 and S/C=2.

For recycled granitic sand, the porosity was consistently higher across comparable mix proportions. At 0% Al, the porosity ranged from 9.5 to 22.7%. At 0.5% Al, the porosity increased to 12.3–23.6%, and reached 13–25.5% at 1% Al. The highest value across all GS formulations was 25.5% at W/C=1.2, S/C=2, and 1% Al. High porosity was also observed at S/C=3 (up to 21.50%), indicating that the W/C and Al dosages governed pore development consistently across all S/C ratios tested.



	W/C=0,7 S/C=4	W/C=0,6	W/C=0,8 S/C=3	W/C=1	W/C=0,6	W/C=0,8 S/C=2	W/C=1	W/C=1,2
0	9.90	8.30	12.50	16.80	9.80	17.00	17.80	23.80
0,5	10.90	9.80	16.00	16.70	13.20	20.30	23.80	21.70
1	11.60	11.00	18.60	17.60	14.60	21.60	22.40	25.20

Figure 7: Porosity with natural sand



	W/C=0,7 S/C=4	W/C=0,8	W/C=1 S/C=3	W/C=0,6	W/C=0,8	W/C=1 S/C=2	W/C=1,2
0	11.80	15.90	19.70	9.50	17.80	22.70	22.20
0,5	12.30	19.20	21.90	18.50	19.70	23.60	23.50
1	16.00	19.70	21.50	13.00	21.00	23.60	25.50

Figure 8: Porosity with granitic sand

Mechanical Properties

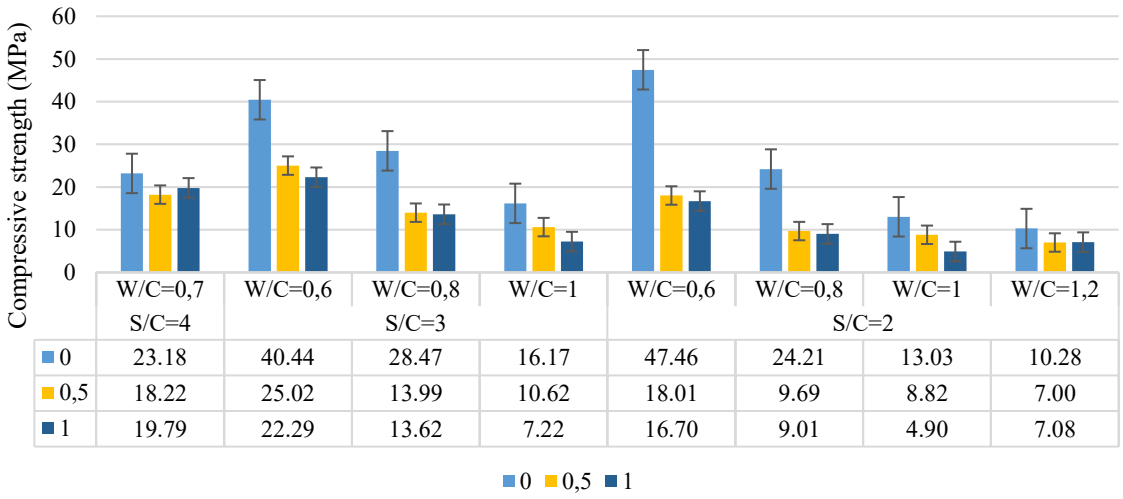
Evolution of compressive strength

The compressive strength decreased with increasing aluminum powder dosage and higher W/C ratios for both sand types (Figure 9 and Figure 10). The control mixtures (0% Al) exhibited the highest strengths in all series, whereas the mixtures with 1% Al exhibited the lowest values.

For natural sand, the compressive strength at 0% Al ranged from 10.28 MPa (W/C=1.2, S/C=2) to 47.46 MPa (W/C=0.6, S/C=2). At 0.5% Al, the strength decreased to 8.82–25.02 MPa, and further decreased to 4.9–22.29 MPa at 1% Al. At W/C=1.2 and S/C=2, the decrease from 10.28 MPa (0%) to 7.08 MPa (1%) represents a 31% reduction.

For recycled granitic sand, the strength at 0% Al ranged from 11.81 to 49.16 MPa, with the maximum again at W/C=0.6 and S/C=2. At 0.5% Al, the strength decreased to 2.91–20.83 MPa, and to 2.44–16.67 MPa at 1% Al. The minimum strength across all GS mixes was 2.44 MPa at W/C=1.2, S/C=2, and 1% Al, representing an 84% reduction from the 0% Al reference of 15.5 MPa at the same W/C and S/C.

At 0% Al, granitic sand produced higher compressive strengths than natural sand at low W/C ratios (e.g., 49.16 vs. 47.46 MPa at W/C=0.6, S/C=2). However, with the addition of aluminum, GS suffers sharper absolute and relative strength losses. At high W/C ratios and 1% Al, natural sand exhibited better compressive performance.



	W/C=0,7 S/C=4	W/C=0,6 S/C=3	W/C=0,8 S/C=3	W/C=1 S/C=3	W/C=0,6 S/C=2	W/C=0,8 S/C=2	W/C=1 S/C=2	W/C=1,2 S/C=2
0	23.18	40.44	28.47	16.17	47.46	24.21	13.03	10.28
0,5	18.22	25.02	13.99	10.62	18.01	9.69	8.82	7.00
1	19.79	22.29	13.62	7.22	16.70	9.01	4.90	7.08

Figure 9: Compressive strength with natural sand

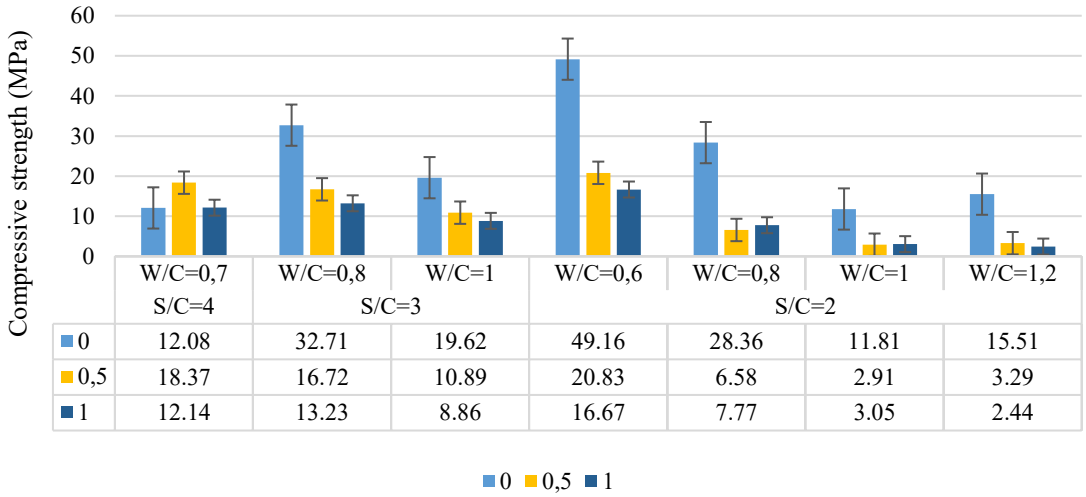


Figure 10: Compressive strength with granitic sand

Evolution of flexural strength

The flexural strength followed the same general decreasing trend with increasing aluminum dosage and W/C ratio for both sand types (Figure 11 and Figure 12). The mixtures without aluminum (0%) presented the highest flexural strengths, and those with 1% Al presented the lowest.

For natural sand, the flexural strength at 0% Al ranged from 2.50 MPa (W/C=1.2, S/C=2) to 7.65 MPa (W/C=0.6, S/C=2). At 0.5% Al, the values ranged from 2.81 to 6.63 MPa, and 1.92–6.49 MPa at 1% Al. An anomalous evolution was recorded at W/C=1.2 and S/C=2, where the flexural strength increased from 2.50 MPa (0% Al) to 3.91 MPa (1% Al).

For recycled granitic sand, the flexural strength at 0% Al ranged from 3.79 to 7.48 MPa. At 0.5% Al, the range was 2.82–6.50 MPa, and at 1% Al, the values spanned 2.15–6.90 MPa. The highest flexural strength among all the Al-containing mixtures was 6.90 MPa at W/C=0.6, S/C=2, and 1% Al.

At W/C ratios of 0.6–0.8, the flexural strength of the concrete with granitic sand was slightly higher than that of the concrete with natural sand. At higher W/C values and 1% Al, both materials converged to similar levels.

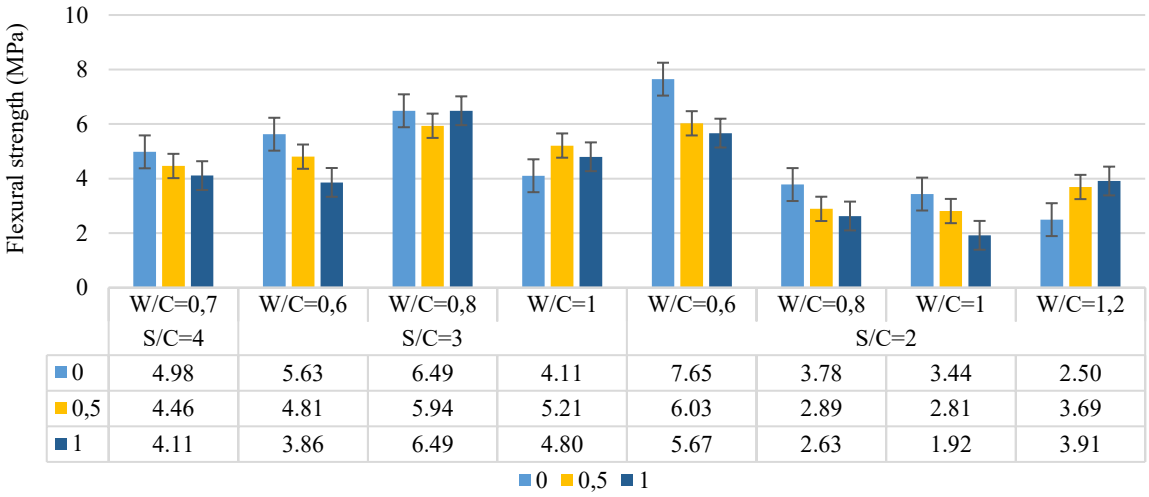


Figure 11: Flexural strength with natural sand

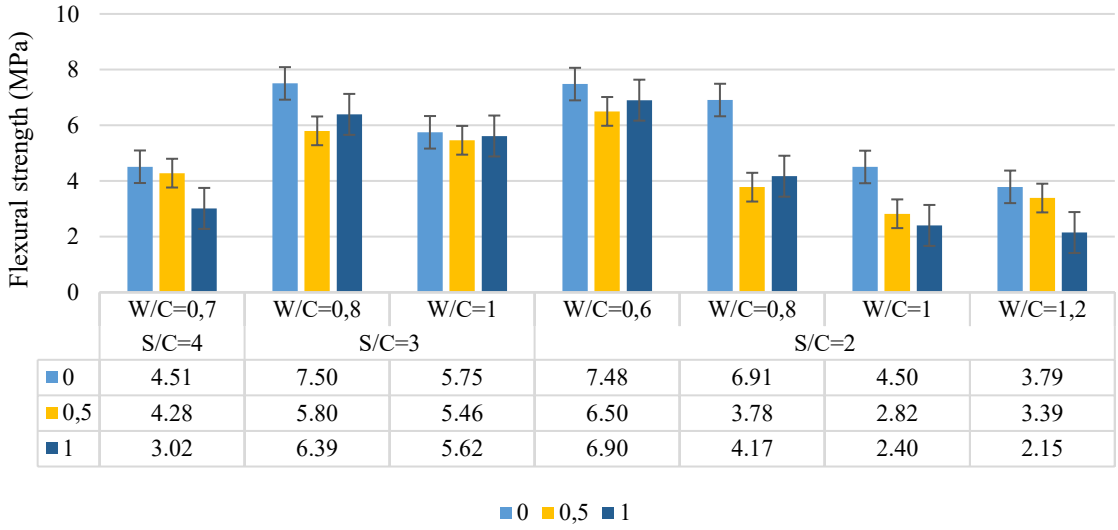


Figure 12: Flexural strength with granitic sand

Thermal Properties

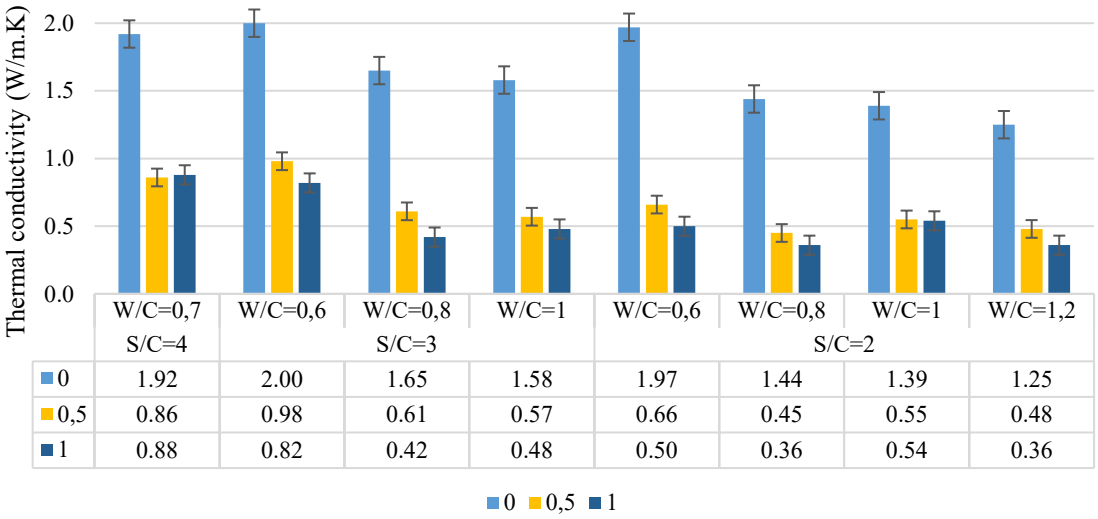
Evolution of thermal conductivity

The thermal conductivity decreased systematically with increasing aluminum content for both sand types (Figure 13 and Figure 14). The lowest conductivity values were recorded at 1% Al across all mix proportions.

For natural sand, the conductivity values for the control ranged from 1.25 to 2 W/m· K. At 0.5% Al, the conductivity decreased to 0.45–0.98 W/m·K and decreased further to 0.36–0.88 W/m·K at 1%. At W/C=1.2 and S/C=2, the conductivity decreased from 1.25 W/m·K (0%) to 0.36 W/m·K (1%), a reduction of 71%.

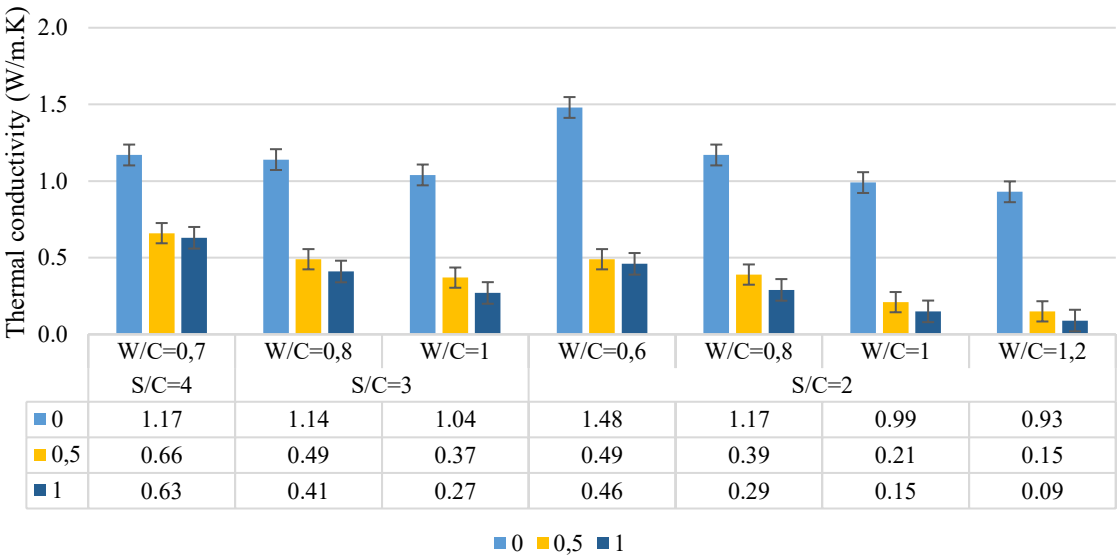
For recycled granitic sand, the conductivity values for the control ranged from 0.93 to 1.48 W/m·K. With 0.5% aluminum, the conductivity decreased to 0.15–0.66 W/m·K and reached 0.09–0.5 W/m·K at 1%. The minimum value across all formulations was 0.09 W/m·K, at W/C=1.2, S/C=2, and 1% aluminum, representing a 90% reduction from the 0% Al reference of 0.93 W/m·K.

For equivalent mix proportions and aluminum content, the granitic sand consistently produced a lower thermal conductivity than the natural sand. The difference increased with the aluminum content and was most pronounced at high W/C and low S/C ratios.



	W/C=0,7 S/C=4	W/C=0,6 S/C=3	W/C=0,8 S/C=3	W/C=1 S/C=3	W/C=0,6 S/C=2	W/C=0,8 S/C=2	W/C=1 S/C=2	W/C=1,2 S/C=2
0	1.92	2.00	1.65	1.58	1.97	1.44	1.39	1.25
0,5	0.86	0.98	0.61	0.57	0.66	0.45	0.55	0.48
1	0.88	0.82	0.42	0.48	0.50	0.36	0.54	0.36

Figure 13: Conductivity with natural sand



	W/C=0,7 S/C=4	W/C=0,8 S/C=3	W/C=1 S/C=3	W/C=0,6 S/C=2	W/C=0,8 S/C=2	W/C=1 S/C=2	W/C=1,2 S/C=2
0	1.17	1.14	1.04	1.48	1.17	0.99	0.93
0,5	0.66	0.49	0.37	0.49	0.39	0.21	0.15
1	0.63	0.41	0.27	0.46	0.29	0.15	0.09

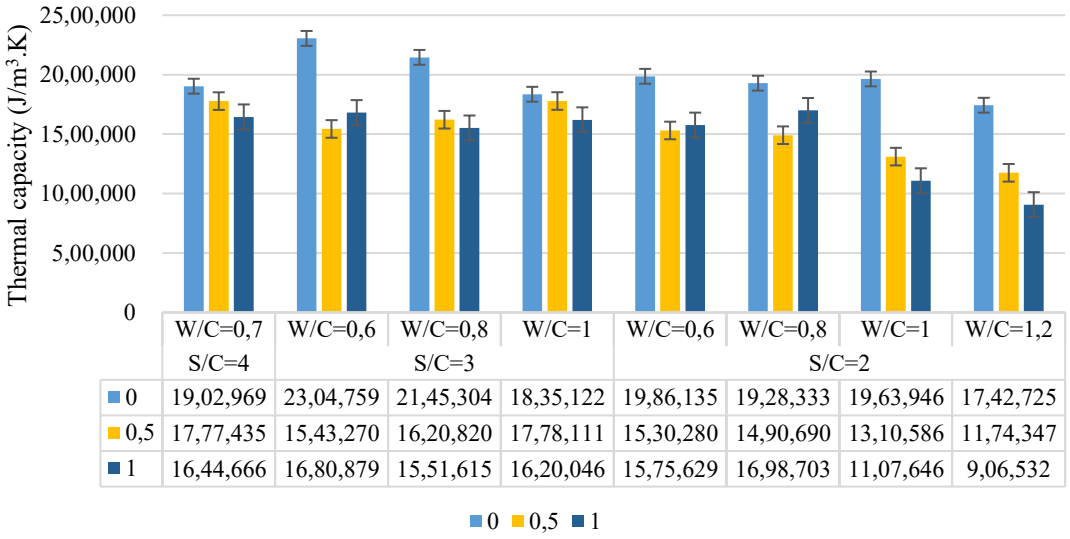
Figure 14: Thermal conductivity with granitic sand

Evolution of thermal capacity

The thermal capacity decreased as the aluminum content increased from 0 to 1% for both sand types (Figure 15 and Figure 16). This decrease was observed across all W/C and S/C ratios, although its magnitude varied with the mix proportions.

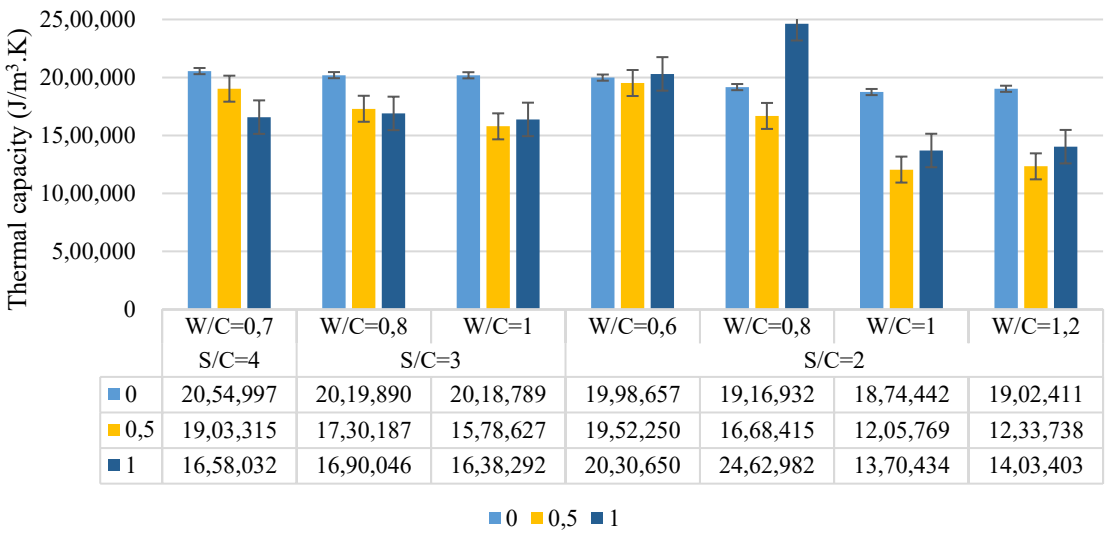
For natural sand, the control mixtures showed thermal capacity values of 1.74×10^6 to 2.30×10^6 J/m³· K. At 0.5% Al, values ranged in 1.31×10^6–1.78×10^6 J/m³·K, and 0.91×10^6–1.68×10^6 J/m³·K at 1% Al. The largest absolute decrease was observed at W/C=1.2 and S/C=2, decreasing from 1.74×10^6 J/m³·K (0%) to 0.91×10^6 J/m³·K (1%).

For recycled granitic sand, the control values ranged from 1.87×10^6 to 2.05×10^6 J/m³· K. At 1% Al, the range extended from 1.37×10^6 to 2.46×10^6 J/m³· K. The maximum thermal capacity across all designs was 2.46×10^6 J/m³·K, at W/C=0.8, S/C=2, and 1% Al. In all cases, the GS formulations maintained higher thermal capacity values than the corresponding NS formulations at equivalent Al dosages.



	W/C=0,7 S/C=4	W/C=0,6 S/C=3	W/C=0,8 S/C=3	W/C=1 S/C=3	W/C=0,6 S/C=2	W/C=0,8 S/C=2	W/C=1 S/C=2	W/C=1,2 S/C=2
0	19,02,969	23,04,759	21,45,304	18,35,122	19,86,135	19,28,333	19,63,946	17,42,725
0,5	17,77,435	15,43,270	16,20,820	17,78,111	15,30,280	14,90,690	13,10,586	11,74,347
1	16,44,666	16,80,879	15,51,615	16,20,046	15,75,629	16,98,703	11,07,646	9,06,532

Figure 15: Heat capacity with natural sand



	W/C=0,7 S/C=4	W/C=0,8 S/C=3	W/C=1 S/C=3	W/C=0,6 S/C=2	W/C=0,8 S/C=2	W/C=1 S/C=2	W/C=1,2 S/C=2
0	20,54,997	20,19,890	20,18,789	19,98,657	19,16,932	18,74,442	19,02,411
0,5	19,03,315	17,30,187	15,78,627	19,52,250	16,68,415	12,05,769	12,33,738
1	16,58,032	16,90,046	16,38,292	20,30,650	24,62,982	13,70,434	14,03,403

Figure 16: Heat capacity with granitic sand

DISCUSSION

Swelling, Porosity, and Density Relationships

Swelling increased sharply with the aluminum content for both sand types and was amplified by higher W/C and lower S/C ratios and higher cement content (Dhasindrakrishna et al., 2021)(Shabbar et al., 2017). This behavior reflects the high formation of hydrogen as a more alkaline pore solution becomes available to react with Al. This result agrees with the literature on Al-foamed lightweight aerated concrete, where the W/C ratio is identified as the primary driver of the volumetric expansion amplitude(Shabbar et al., 2017)(Maza et al., 2023). At 1% Al and W/C = 1.2, S/C = 2, natural sand reached a maximum swelling of 65.22%, whereas granitic sand reached 63.33%, within the upper range reported for chemically foamed cement systems using similar Al dosages (Talebi et al., 2020).

Although granitic sand produced comparable swelling to natural sand, it had a lower density than natural sand. The minimum density of 1003 kg/m³ for GS and 1168 kg/m³ for NS (W/C = 1.2, S/C = 2, 1% Al) agree with the values (350–1850 kg/m³) in the literature on lightweight concrete (Liu et al., 2024)(Abdellatief et al., 2024).

Water-accessible porosity followed the same pattern, reaching up to 25.5% for GS and 25.2% for NS, both at W/C = 1.2 and S/C = 2 with 1% Al. These values are characteristic of open-pore structures formed by chemical foaming without autoclave treatment (Liu et al., 2024)(Chen et al., 2021). The swelling-porosity-density relationships confirmed the synergistic effect of granitic sand with Al foaming to form a more developed pore network. This could

have been further improved if the fine in the granitic sand was used for its microfiller potential in cellular systems (Zafar et al., 2020)(Saxena et al., 2022).

Physical and Mechanical Performance Relationships

The compressive and flexural strengths decreased systematically with decreasing density for both sand types and all mix proportions, consistent with the well-established porosity-strength relationship in foam concrete (Liu et al., 2024)(Al-Ani et al., 2025). This behavior is governed by the progressive reduction in the load-bearing solid cross-section as the pore fraction increases. The decrease in strength is particularly significant in Al-foamed non-autoclaved systems, where the pores are interconnected rather than spherically closed (Shabbar et al., 2017). In the present study, the increase in Al from 0% to 1% reduced the compressive strength by 84% with GS (15.5 to 2.4 MPa at W/C = 1.2, S/C = 2) and 31% with NS (10.3 to 7.1 MPa). At low W/C ratios (0.6–0.8) and without aluminum addition, GS produced slightly higher compressive strengths than NS (49.16 vs. 47.46 MPa at W/C = 0.6, S/C = 2). This initial strength advantage can be attributed to the limited microfiller effect attributed to granite fines, which densify the interfacial transition zone and reduce porosity (Saxena et al., 2022)(Gupta & Vyas, 2018). However, GS exhibited a sharper decrease in strength as Al content increased, possibly due to its pore structure. This tradeoff between the quality of the control matrix and structural vulnerability at high porosities is a key characteristic of finely graded mineral fillers in foamed systems.

The compressive values for the optimized low-Al formulations (above 20 MPa) were adequate for low-load-bearing wall applications. With 1% Al, the 2.4-7.1 MPa range does not allow these mortars structural application, but rather for insulation applications.

Physical and Thermal Performance Relationships

Thermal conductivity (TC) decreased significantly with increasing Al dosage as did the associated density, confirming that pore volume fraction is the dominant control on heat transfer (Liu et al., 2024)(Chen et al., 2021). For NS, conductivity decreased from a maximum of 2 W/m.K (0% Al, high S/C) to a minimum of 0.36 W/mK (1% Al, W/C = 1.2, S/C = 2), a reduction of 71%. These values span the transition from ordinary mortar behavior to the insulating range, in line with published data for foam concrete density between 1100 and 1800 kg/m³ (Liu et al., 2024). GS achieved more significant reductions, 90% (from 0.09 to 0.93 W/m·K at W/C=1.2, S/C=2), within the ultra-insulating class of foam concrete (< 0.1 W/m. K) (Mohamed et al., 2024)(Chen et al., 2021). This high reduction of GS can be explained by two mechanisms: the distribution of nucleation sites more homogeneously, producing more close

pores (Dhasindrakrishna et al., 2021)(Zafar et al., 2020). More uniform pore size distribution reduces radiative and conductive heat transfer through the gas phase more effectively than coarser, less uniform pore networks, as demonstrated by Chen et al. (Chen et al., 2021) in pore-structure of AAC. However, this hypothesis needs to be confirmed by pore structure analysis.

The thermal capacity showed an inverse evolution to TC. It decreases as porosity increases, from approximately 1.87–2.05 × 10^6 J/m^3.K at 0% Al to 1.37–2.46 × 10^6 J/m^3.K at 1% Al with GS, and more sharply from 1.74–2.30 × 10^6 to 0.91–1.68 × 10^6 J/m^3.K with NS. The consistently higher heat storage capacity of GS, even at maximum porosity, suggests that granite maintains a more continuous solid phase around pores, which is a pore-wall densification effect, as reported for mineral waste fillers in AAC (Abhilasha et al., 2023)(Chen et al., 2021). A higher thermal capacity moderates indoor temperature fluctuations independently of conductivity, which is a critical performance criterion for the Sudano-Sahelian context with a high diurnal temperature amplitude (Hema et al., 2021). Therefore, the combination of low conductivity and comparatively preserved heat storage capacity in GS mortars positions them as thermally superior candidates for envelope applications in hot climates.

Furthermore, the relationship between the thermal conductivity and bulk density was modelled separately for each sand type using a power law of the form $\lambda = \alpha*(\rho/1000)^n$. For NS, the fitted equation is $\lambda = 0.220*(\rho/1000)^{2.55}$ ($R^2 = 0.75$), and for GS, $\lambda = 0.0875*(\rho/1000)^{3.68}$ ($R^2 = 0.95$). Both exponents fall within the range reported for chemically foamed and lightweight cementitious systems (n = 1.5–3.5), confirming that the pore volume fraction is the dominant control on heat transfer in these materials. The higher exponent for GS (3.68 vs. 2.55) indicates that the thermal conductivity in the GS formulations is more sensitive to density reduction. For instance, a 30% reduction in density corresponds to a 66% decrease in λ for GS but only a 52% decrease for NS. The lower prefactor for GS (α = 0.0875 vs. 0.220) further indicates that, at equivalent density, GS mortars are intrinsically less conductive than NS mortars, reflecting both the lower conductivity of the granite aggregate and the more closed pore structure it promotes.

CONCLUSION

This study evaluated the physical, mechanical, and thermophysical properties of aluminum-based cellular mortars incorporating natural sand (NS) and recycled granitic sand (GS) across varying aluminum powder dosages (0%, 0.5%, 1%), sand-to-cement ratios (S/C = 2, 3, 4), and water-to-cement ratios (W/C = 0.6 to 1.2).

Physical properties such as swelling, porosity, and density evolved consistently with all three mixing variables. Increasing the aluminum dosage and W/C ratio progressively expanded the

pore network, with water-accessible porosity ranging from 8% to 26% across all formulations. Linear swelling reached 65.22% (NS) and 63.33% (GS). Bulk density was reduced by 44% from 1785 to 1003 kg/m³ with GS and by 35% from 1796 to 1168 kg/m³ with NS at W/C = 1.2, S/C = 2, and 1% Al. The minimum density achieved, 1003 kg/m³ with GS, confirms that these mortars are genuinely lightweight materials. Under equivalent conditions, GS exhibited higher swelling and porosity and lower density than NS.

Mechanical properties, in terms of compressive and flexural strength, decreased with increasing porosity, confirming that these mortars are suitable for non-structural and insulating applications. Compressive strength ranged from 2.4 to 49 MPa and flexural strength from 1.9 to 7.6 MPa across all formulations. GS showed a marginal initial strength advantage at low W/C (49.16 vs. 47.46 MPa at W/C = 0.6, S/C = 2, 0% Al), but suffered sharper losses as aluminum increased, reaching a reduction of 84% from 15.5 to 2.4 MPa, against 31% from 10.3 to 7.1 MPa for NS, at W/C = 1.2, S/C = 2, and 1% Al. Optimized low-Al, low-W/C designs remain adequate for non-load-bearing wall construction, while high-Al mixes serve thermal insulation purposes. NS retained better mechanical performance at high porosity.

Thermal properties showed substantial improvements with increasing pore volume, with GS consistently outperforming NS. Thermal conductivity reductions reached 90% from 0.93 to 0.09 W/m·K with GS, and 71% from 1.25 to 0.36 W/m·K with NS, at W/C = 1.2, S/C = 2, and 1% Al. Across all mix proportions, the absolute maximum reduction reached 94%, from 2 to 0.09 W/m·K. The most porous GS designs reached the ultra-insulating range (< 0.1 W/m·K), making them relevant candidates for envelope applications in the hot and dry Sudano-Sahelian climate. Thermal capacity also decreased with porosity but remained consistently higher in GS than NS at equivalent dosages. This combination of low conductivity and preserved heat storage capacity positions GS formulations as thermally superior for envelope applications exposed to high diurnal temperature amplitudes.

Overall, GS favored thermal efficiency, whereas NS favored structural performance, and a balance between both was achieved by adjusting the Al dosage and W/C ratio. The use of recycled granite waste supports more sustainable construction practices in regional contexts.

Future investigations should explore the substitution or partial replacement of Portland cement with low-carbon binders such as geopolymers, LC3 (limestone calcined clay cement), or lime-rich industrial by-products, as well as the use of recycled aluminum from post-consumer beverage cans as an alternative foaming agent to further reduce the embodied carbon of these mortars. Long-term durability testing under Sudano-Sahelian exposure conditions, including wetting-drying cycles, is also recommended. Finally, lifecycle assessment (LCA) and lifecycle

energy analysis (LCE) at the construction and operational scales are needed to quantify the environmental and energy gains of these cellular mortars when deployed in actual building envelopes.

Funding Statement: The study did not receive fund.

Acknowledgement: The data collected was assisted by the laboratory technicians

Data Access Statement: Research data supporting this publication are available upon request.

Conflict of Interest declaration: The authors declare that they have no affiliations with or involvement in any organization or entity with any financial interest in the subject matter or materials discussed in this manuscript.

Author Contributions: PN and AM contributed to the design and implementation of the research, PN, YBT, AO, MNC, NS and AM to the analysis of the results and to the writing of the manuscript. AM conceived the original and supervised the project.

REFERENCES

Abdellatief, M., Ahmed, Y. M., Taman, M., Elfadaly, E., Tang, Y., & Abadel, A. A. (2024). Physico-mechanical, thermal insulation properties, and microstructure of geopolymer foam concrete containing sawdust ash and egg shell. *Journal of Building Engineering*, *90*, 109374. https://doi.org/10.1016/J.JOBE.2024.109374

Abhilasha, Kumar, R., Lakhani, R., Mishra, R. K., & Khan, S. (2023). Utilization of Solid Waste in the Production of Autoclaved Aerated Concrete and Their Effects on its Physio-mechanical and Microstructural Properties: Alternative Sources, Characterization, and Performance Insights. *International Journal of Concrete Structures and Materials*, *17*(1), 6-. https://doi.org/10.1186/S40069-022-00569-X/FIGURES/9

Akkouri, N., Bourzik, O., Baba, K., & Tayeh, B. A. (2022). Thermophysical characteristics of eco-friendly mortars containing recycled PET as partial sand replacement in dry and wet conditions. *Innovative Infrastructure Solutions*, *7*(4), 238-. https://doi.org/10.1007/S41062-022-00838-4/METRICS

Al Ismaeel, A., Alzlfawi, A., Ahmad, J., & Qureshi, H. J. (2026). Granite powder in concrete: a review on durability and microstructural properties. *REVIEWS ON ADVANCED MATERIALS SCIENCE*, *65*(1). https://doi.org/10.1515/RAMS-2025-0179/ASSET/GRAPHIC/J_RAMS-2025-0179_FIG_022.JPG

Al-Ani, H. K. K., Hilal, A. A., & Hama, S. M. (2025). Characteristics of Fresh and Hardened Sustainable Foamed Concrete for Structural Applications. *Journal of*

Engineering, *2025*(1), 2998605. https://doi.org/10.1155/JE/2998605

Chen, G., Li, F., Jing, P., Geng, J., & Si, Z. (2021). Effect of Pore Structure on Thermal Conductivity and Mechanical Properties of Autoclaved Aerated Concrete. *Materials 2021, Vol. 14, Page 339*, *14*(2), 339. https://doi.org/10.3390/MA14020339

Dhasindrakrishna, K., Ramakrishnan, S., Pasupathy, K., & Sanjayan, J. (2021). Collapse of fresh foam concrete: Mechanisms and influencing parameters. *Cement and Concrete Composites*, *122*, 104151. https://doi.org/10.1016/J.CEMCONCOMP.2021.104151

Ganesan, S., Othuman Mydin, M. A., Mohd Yunos, M. Y., & Mohd Nawi, M. N. (2015). Thermal Properties of Foamed Concrete with Various Densities and Additives at Ambient Temperature. *Applied Mechanics and Materials*, *747*, 230–233. https://doi.org/10.4028/www.scientific.net/amm.747.230

Gencel, O., Yavuz Bayraktar, O., Kaplan, G., Arslan, O., Nodehi, M., Benli, A., Gholampour, A., & Ozbakkaloglu, T. (2022). Lightweight foam concrete containing expanded perlite and glass sand: Physico-mechanical, durability, and insulation properties. *Construction and Building Materials*, *320*, 126187. https://doi.org/10.1016/J.CONBUILDMAT.2021.126187

Gupta, L. K., & Vyas, A. K. (2018). Impact on mechanical properties of cement sand mortar containing waste granite powder. *Construction and Building Materials*, *191*, 155–164. https://doi.org/10.1016/J.CONBUILDMAT.2018.09.203

Habsya, C., Diharjo, K., Setyono, P., & Satwiko, P. (2018). Physical, mechanical and thermal properties of lightweight foamed concrete with fly ash. *IOP Conference Series: Materials Science and Engineering*, *420*(1). https://doi.org/10.1088/1757-899X/420/1/012062

Hema, C., Messan, A., Lawane, A., & Van Moeseke, G. (2020). Impact of the Design of Walls Made of Compressed Earth Blocks on the Thermal Comfort of Housing in Hot Climate. *Buildings*, *10*(9), 157. https://doi.org/10.3390/buildings10090157

Hema, C., Soro, D., Nshimiyimana, P., Lawane, A., Messan, A., & Van Moeseke, G. (2021). Improving the thermal comfort in hot region through the design of walls made of compressed earth blocks: an experimental investigation. *Journal of Building Engineering*, *38*, 102148. https://doi.org/https://doi.org/10.1016/j.jobe.2021.102148

Karri, J. G., Yenurkar, P. A., & Tondhre, K. D. (2018). *Use of Aluminum Powder To Create Light Weight Blocks- A Review*. 1–5.

Liu, Y., Zhao, Z., Amin, M. N., Ahmed, B., Khan, K., Arifeen, S. U., & Althoey, F. (2024).

Foam concrete for lightweight construction applications: A comprehensive review of the research development and material characteristics. *Reviews on Advanced Materials Science*, *63*(1). https://doi.org/10.1515/RAMS-2024-0022/ASSET/GRAPHIC/J_RAMS-2024-0022_FIG_011.JPG

Maza, M., Tebbal, N., Rahmouni, Z. E. A., Maza, M., Tebbal, N., & Rahmouni, Z. E. A. (2023). Effect of Aluminum Waste on Mortar Thermo-Mechanical Behavior. *International Review of Civil Engineering (IRECE)*, *14*(5), 415–424. https://doi.org/10.15866/IRECE.V14I5.22951

Mohamed, A. M., Tayeh, B. A., Majeed, S. S., Aisheh, Y. I. A., & Salih, M. N. A. (2024). Ultra-light foamed concrete mechanical properties and thermal insulation perspective: A comprehensive review. *Journal of CO2 Utilization*, *83*, 102827. https://doi.org/10.1016/J.JCOU.2024.102827

Nouhoun, I. S., Nshimiyimana, P., Hema, C., & Messan, A. (2025). Development of a Life Cycle Inventory Database for Environmental Impact Assessment of Construction Materials in Burkina Faso. *Sustainability*, *17*(2), 471. https://doi.org/10.3390/su17020471

Nshimiyimana, P., Adufu, Y. D., Savadogo, N., Kanazoe, K., Kindo, M., & Messan, A. (2025). Towards the development of eco-cement containing furnace slag from the recycling of metal scraps into steel in Burkina Faso. *MRS Advances*, *in press*. https://doi.org/10.1557/s43580-025-01328-2

Ouédraogo, A. L., Kabré, S., Malbila, E., Compaoré, A., Saré, R., Ilboudo, P., Kam, S., Korgo, B., Bathiebo, D. J., Kieno, F. P., & Blanchard, P. (2022). Comparative Study of the Thermal and Mechanical Properties of Foamed Concrete with Local Materials. *World Journal of Engineering and Technology*, *10*(3), 550–564. https://doi.org/10.4236/WJET.2022.103035

Ouedraogo, A. L. S. N., Messan, A., Yamegueu, D., & Coulibaly, Y. (2022). A model for thermal comfort assessment of naturally ventilated housing in the hot and dry tropical climate. *International Journal of Building Pathology and Adaptation*, *40*(2), 183–201. https://doi.org/10.1108/IJBPA-02-2021-0011

Prozuments, A., Ménézo, C., Orumwense, E., Kahn, M. T., Nguewo, D. Y., Hema, C., Nshimiyimana, P., N'tsoukpoe, K. E., Messan, A., Borodinecs, A., & Desta, A. F. (2025). Assessment of Indoor Thermal Comfort Criteria and Challenges Across the African continent. *Journal of Sustainable Architecture and Civil Engineering*, *38*(2), 161–176. https://doi.org/10.5755/j01.sace.38.2.40349

Ramadji, C., Messan, A., & Prud'homme, E. (2020). Influence of granite powder on physico-mechanical and durability properties of mortar. *Materials*, *13*(23), 1–22. https://doi.org/10.3390/ma13235406

Saxena, R., Gupta, T., Sharma, R. K., & Siddique, S. (2022). Mechanical, durability and microstructural assessment of geopolymer concrete incorporating fine granite waste powder. *Journal of Material Cycles and Waste Management*, *24*(5), 1842–1858. https://doi.org/10.1007/S10163-022-01439-0

Shabbar, R., Nedwell, P., & Wu, Z. (2017). Mechanical properties of lightweight aerated concrete with different aluminium powder content. *MATEC Web of Conferences*, *120*, 02010. https://doi.org/10.1051/matecconf/201712002010

Talebi, H. R. A. K., Kayan, B. A., Asadi, I., & Hassan, Z. F. A. (2020). Investigation of Thermal Properties of Normal Weight Concrete for Different Strength Classes. *J. Environ. Treat. Tech*, *8*, 908–914. https://www.researchgate.net/publication/342211680_Investigation_of_Thermal_Properties_of_Normal_Weight_Concrete_for_Different_Strength_Classes

UN-Habitat. (2022). *World cities report 2022 : envisaging the future of cities*. https://digitallibrary.un.org/record/3984713

Zafar, M. S., Javed, U., Khushnood, R. A., Nawaz, A., & Zafar, T. (2020). Sustainable incorporation of waste granite dust as partial replacement of sand in autoclave aerated concrete. *Construction and Building Materials*, *250*, 118878. https://doi.org/10.1016/J.CONBUILDMAT.2020.118878